Nanodiscs

Deutsche Ausgabe: DOI: 10.1002/ange.201705569
Internationale Ausgabe: DOI: 10.1002/anie.201705569

Bioinspired, Size-Tunable Self-Assembly of Polymer–Lipid Bilayer Nanodiscs

*Thirupathi Ravula, Sudheer Kumar Ramadugu, Giacomo Di Mauro, and Ayyalusamy Ramamoorthy**

Abstract: *Polymer-based nanodiscs are valuable tools in biomedical research that can offer a detergent-free solubilization of membrane proteins maintaining their native lipid environment. Herein, we introduce a novel ca. 1.6 kDa SMA-based polymer with styrene:maleic acid moieties that can form nanodiscs containing a planar lipid bilayer which are useful to reconstitute membrane proteins for structural and functional studies. The physicochemical properties and the mechanism of formation of polymer-based nanodiscs are characterized by light scattering, NMR, FT-IR, and TEM. A remarkable feature is that nanodiscs of different sizes, from nanometer to sub-micrometer diameter, can be produced by varying the lipid-to-polymer ratio. The small-size nanodiscs (up to ca. 30 nm diameter) can be used for solution NMR spectroscopy studies whereas the magnetic-alignment of macro-nanodiscs (diameter of > ca. 40 nm) can be exploited for solid-state NMR studies on membrane proteins.*

The search for membrane mimetic soft nanomaterials that provide native environment for structural and functional studies of membrane proteins has been a formidable challenge.[1–3] A breakthrough was provided by nanodiscs, which were inspired from a high-density lipoprotein (HDL).[3–5] Nanodiscs are disc-shaped patches of lipid bilayers surrounded by an amphiphilic belt and represent an excellent model system offering a great stability and control of oligomeric states of the reconstituted membrane protein.[6] Nanodisc technology can be used for isolation, purification, structural and functional characterization of membrane proteins, and is increasingly utilized.[3] The amphiphilic belt is critical for the stability and function of nanodiscs. Studies have reported different types of surrounding belts including membrane scaffold proteins (MSPs),[5,7] peptides,[8] and polymer.[9] Even though MSP-based nanodiscs are excellent mimics of the membrane, the reconstitution of a membrane protein still requires the undesirable use of detergents,[10] and therefore detergent-free solubilization of membrane proteins attracted new attention in the field.[11,12]

[*] Dr. T. Ravula, Dr. S. K. Ramadugu, G. Di Mauro, Prof. A. Ramamoorthy
Biophysics Program and Department of Chemistry
The University of Michigan
Ann Arbor, MI 48109-1055 (USA)
E-mail: ramamoor@umich.edu
Supporting information and the ORCID identification number(s) for the author(s) of this article can be found under: https://doi.org/10.1002/anie.201705569.

Recently reported studies have shown that hydrolyzed styrene:maleic acid (SMA) copolymer can be used to form nanodiscs and to extract membrane proteins directly from the cell membrane.[11] Although successful and increasingly utilized for structural studies on membrane proteins, the narrow range of nanodisc size[13] (typically 8 to 15 nm) that can be prepared using SMA is a major limitation for studies on large size proteins or protein–protein complexes. The high expense associated with the large quantity of SMA-based nanodiscs that is needed for biological applications is also a limitation, while there is a need to enhance the tolerance to acidic pH and divalent metal ions.[14]

Herein, we introduce more versatile polymer-based nanodiscs to overcome the limitations of previously reported nanodiscs. Synthesis and characterization of a low-molecular-weight copolymer, amine modified styrene:maleic acid denoted as SMA-EA, and its application to study membrane proteins using solution and solid-state NMR spectroscopy experiments are reported. The ability of SMA-EA copolymer to form defined size nanodiscs, that can easily be controlled by the lipid:polymer ratio, is well demonstrated using static light scattering (SLS), dynamic light scattering (DLS), size-exclusion chromatography (SEC), Fourier-transform infrared spectroscopy (FT-IR), solid-state nuclear magnetic resonance (ssNMR), transmission electron microscopy (TEM), and fluorescence experiments. Most importantly, we show that SMA-EA polymers can form large size nanodiscs (called "macro-nanodiscs") that can spontaneously align in the presence of an external magnetic field and the direction of alignment can be altered using a paramagnetic salt. These nanodiscs and macro-nanodiscs can be used to study atomic-resolution structure and dynamics of membrane proteins.

A commercially available, less expensive, low molecular weight ($M_n \approx 1.6$ kDa) approximately 1.3:1 styrene:maleic anhydride copolymer was used as a starting material. Our experiments confirmed that this SMA copolymer by itself cannot be used to prepare nanodiscs (data shown in Supporting Information, Figure S1). To overcome this limitation, we developed a simple two-step synthetic approach to modify the SMA polymer as shown in Figure 1 A. First, the SMA polymer was treated with 2-aminoethanol in the presence of *N*,*N*-trimethylamine, and then followed by the hydrolysis of any unreacted maleic anhydride. Other details on the production of the final product, SMA-EA polymer, are given in the Supporting Information.

The newly synthesized approximately 2 kDa SMA-EA polymer was characterized by FT-IR (Figure 1 B) experiments. The appearance of a characteristic broad band centered around 3300 cm^{-1} in the 3000–3600 cm^{-1} region of

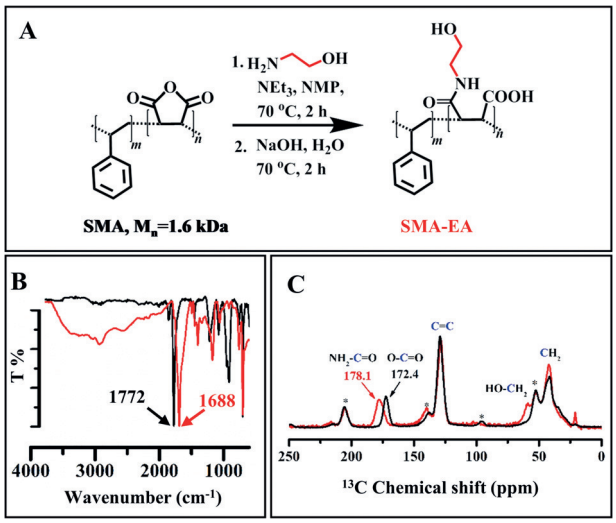

Figure 1. Synthesis and characterization of SMA-EA polymer: A) Reaction scheme for the modification of SMA polymer by an amination reaction. B) FT-IR spectra of SMA (black) and SMA-EA (red; US patent (filed)) polymers showing differences underlying the amination of maleic anhydride. C) ^{13}C CP-MAS NMR spectra of SMA (black) and SMA-EA (red) obtained under 8 kHz spinning further confirm the transformation of SMA to form the SMA-EA polymer; the spinning side bands are indicated by asterisks.

the FT-IR spectrum confirms the formation of SMA-EA polymer; this corresponds to a combination of stretching bands of −OH in the carboxylic and alcoholic groups of SMA-EA. In addition, the formation of amides and complete opening of the anhydride ring of SMA to result in the SMA-EA polymer are indicated by the shift of the 1772 cm^{-1} band observed for SMA to a lower wavenumber 1688 cm^{-1} for SMA-EA.

The SMA-EA polymer was further characterized by ^{13}C cross-polarization magic-angle spinning (CP-MAS) solid-state NMR spectroscopy. By comparing the spectra of SMA-EA and the parent compound SMA (Figure 1C), we were able to assign peaks at 41 and 60 ppm to aliphatic carbons and peaks observed at 128 ppm to aromatic carbons. The peak observed at 172.4 ppm, assigned to the carbonyl carbon of maleic anhydride in SMA, is shifted downfield by 5.7 ppm in the spectrum of SMA-EA suggesting the formation of amides in SMA-EA.

To test the SMA-EA efficacy in solubilizing lipids to form nanodiscs, a solution of the polymer was added to MLVs (multilamellar vesicles) of DMPC (1,2-dimyristoyl-sn-glycero-3-phosphocholine) (1:3 w/w % DMPC:SMA-EA). SMA-EA spontaneously turned the initial cloudy DMPC vesicle solution into a clear transparent solution, indicating the formation of smaller size particles when compared to MLVs of DMPC (Figure 2A). A substantial decrease in the light-scattering intensity over time observed after the addition of SMA-EA polymer to DMPC MLVs suggests that SMA-EA can break large MLVs to form smaller size lipid aggregates. The solubilization of DMPC MLVs into nanodiscs was further characterized by ^{31}P NMR experiments (Figure 2B). The appearance of an isotropic ^{31}P peak ($\delta \approx -2$ ppm) upon the addition of SMA-EA to DMPC MLVs and the increase in the peak intensity with the concentration of SMA-EA suggest the formation of a nanodisc containing a DMPC lipid bilayer that can tumble fast to result in a ^{31}P peak at the isotropic chemical shift frequency (Figure 2B,C). A similar trend was observed by total internal reflection fluorescence (TIRF) microscopy. DMPC vesicles containing 1 mol% of rhodamine-functionalized DMPE were visualized with TIRF as a function of time right after the addition of SMA-EA to DMPC MLVs. As shown in Figure 2D (and in the video in the Supporting Information, Figure S2), the large size MLVs observed before the addition of SMA-EA disappear as the polymer solubilize the vesicles to form small size lipid nanodiscs as observed by a progressive disappearance of the fluorescent signal.

Dynamic light-scattering profiles of nanodiscs at different polymer-to-lipid ratios showed a size distribution profile, indicating that the SMA-EA polymer is able to form stable nanodiscs of different sizes. This result was also confirmed by TEM images (Figure 3B,C).

The interaction between the polymer and lipids in the nanodisc is revealed by the 2D ^{1}H/^{1}H NOESY spectrum (Figures 3D). The cross peaks observed between styrene protons and the DMPC acyl chain's CH_2 protons indicate the interaction between the SMA-EA polymer and DMPC lipid bilayer and suggest a structural model in which the styrene rings are closely located in the hydrophobic core of the DMPC lipid bilayer. The DMPC lipid bilayer within the polymer-based nanodiscs was further investigated using FT-IR experiments. The characteristic sharp peak observed in an FT-IR spectrum due to the CH stretching frequency of

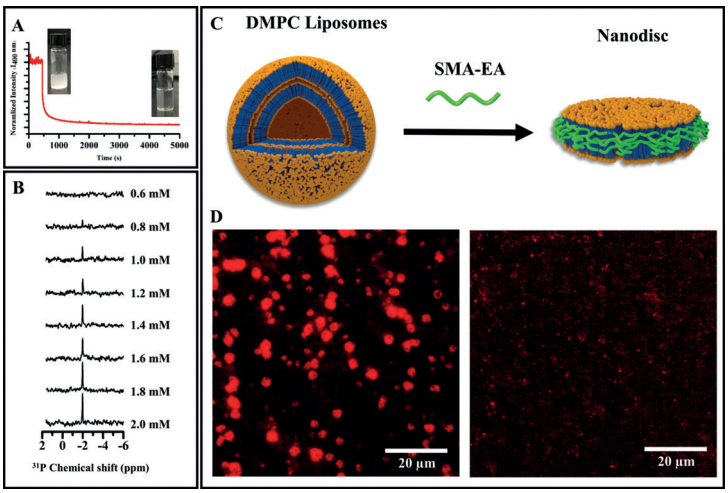

Figure 2. Formation of SMA-EA polymer based nanodiscs: A) Normalized static light scattering of DMPC MLVs upon the addition of SMA-EA polymer. The intense SLS signal observed at time zero ($t = 0$) are due to light scattering by the large-size MLVs decreases over time after the addition of SMA-EA. Inset: photographs of the reaction solutions. B) ^{31}P NMR spectra of DMPC MLVs (5 mM) with the addition of the indicated concentration of SMA-EA polymer. C) Schematic representation of the formation of a SMA-EA nanodisc containing a lipid bilayer. D) TRIF microscope images of DMPC vesicles containing 1 mol% of rhodamine-functionalized DMPE (1,2-Dimyristoyl-sn-glycero-3-phosphoethanolamine) before (left) and after the addition of SMA-EA polymer (right).

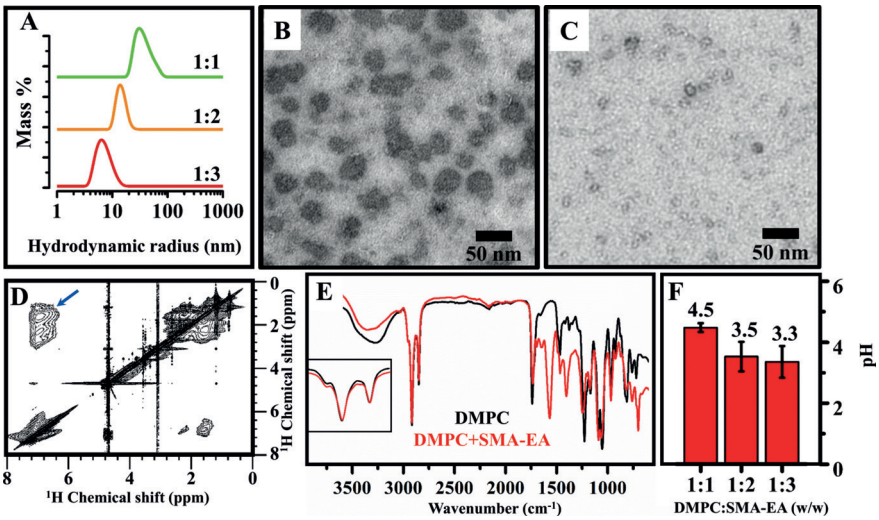

Figure 3. Characterization of SMA-EA polymer based macro- and nanodiscs of DMPC bilayers: A) DLS profiles showing the different size nanodiscs obtained by varying the lipid to polymer molar ratio. B),C) TEM images highlight the difference in the size of nanodiscs obtained by mixing 1:1 (B) or 1:3 (C) ratio of DMPC:SMA-EA (w/w). D) 2D NOESY spectrum of nanodiscs (ca. 10 nm). Blue arrow shows the cross-peaks between styrene ring protons of the SMA-EA polymer and the CH_2 protons of DMPC acyl chains. E) FT-IR spectra of lyophilized DMPC MLVs (black) and nanodiscs containing a DMPC bilayer (red). F) Highest pH for which precipitation of SMA-EA polymer based DMPC lipid nanodiscs were observed by SLS experiments.

DMPC is a good indicator of lipid acyl chains packing in a bilayer. The FT-IR spectra of lyophilized samples of DMPC MLVs and nanodiscs showed no difference in the CH stretching frequencies suggesting a type of lipid packing inside the nanodisc similar to that in liposomes (Figure 3E and see the Supporting Information Figure S3).

One of the disadvantages of SMA polymer nanodiscs is that they tend to precipitate under low pH (<6),[15] which could affect several biochemical protein assays. The stability of SMA-EA nanodiscs under different pH was examined by SLS experiments (see the Supporting Information Figure S5). The results indicate that these nanodiscs are stable under acidic pH up to pH $\approx$ 3.3. Therefore, the SMA-EA polymer based nanodiscs are more tolerant to acidic pH than previously reported polymers. This enhanced stability of SMA-EA nanodiscs is attributed to the reduced number of carboxylic groups when compared to that in the SMA polymer. The nanodisc shows superior stability towards salt (Figure S4) and temperature (Figure S5), and a similar trend was observed in the presence of divalent metal ions (See the Supporting Information Figures S6 and S7).

We then characterized the SMA-EA polymer DMPC nanodiscs (ca. 10 nm in diameter) and macro-nanodiscs (ca. 50 nm in diameter) using NMR spectroscopy. ^{31}P (Figure 4A–C) and ^{14}N (Figure 4D–F) NMR spectra exhibited an isotropic peak (−2.9 ppm) for nanodiscs (Figure 4A,D) while anisotropic peak patterns (Figure 4B E) were observed for macro-nanodiscs indicating their alignment in the presence of an external magnetic field[16,17] (also see Figures S8 and S9). The observation of a peak at −17.9 ppm in the ^{31}P spectrum (Figure 4B) and approximately 8 kHz ^{14}N quadrupole splitting (Figure 4E) suggest that the lipid bilayer normal is oriented perpendicular to the external magnetic field direction. On the other hand, the use of Yb^{3+} ions flipped the orientation of macro-nanodiscs in such a way the bilayer normal became parallel to the magnetic field direction in similar manner to bicelles[18] and therefore

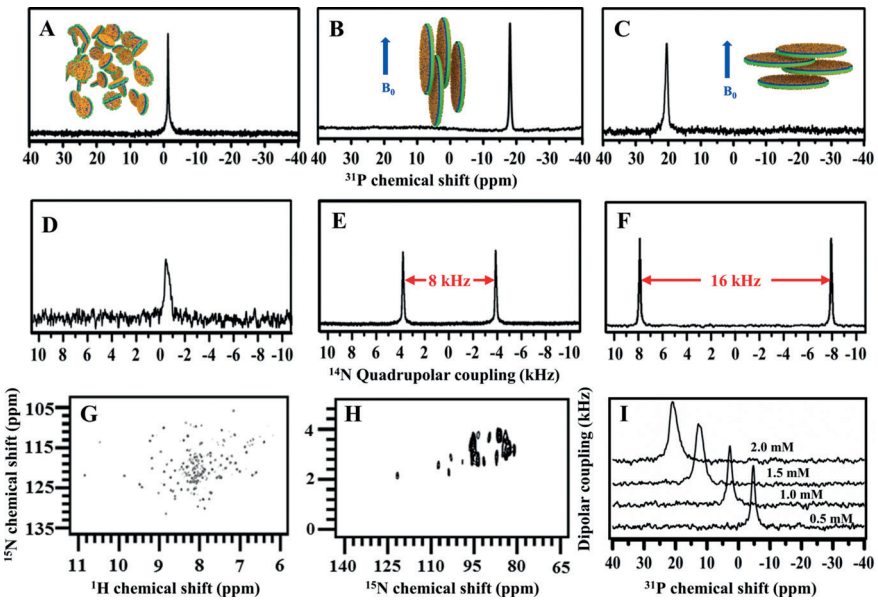

Figure 4. Magnetic-alignment of SMA-EA polymer based macro-nanodiscs: Static ^{31}P (A–C) and ^{14}N (D–F) NMR spectra demonstrate the presence of isotropic nanodiscs (ca. 10 nm diameter) (A,D), the magnetic-alignment of macro-nanodiscs (ca. 50 nm) with the lipid bilayer perpendicular to the external magnetic field (B,E), and flipped macro-nanodiscs in the presence of Yb^{+3} ions with the lipid bilayer parallel to the external magnetic field (C,F). G) 2D ^{15}N–^{1}H TROSY HSQC spectrum of isotropic SMA-EA nanodiscs containing ^{15}N-cytochrome b_5 reconstituted in DMPC lipid bilayers. All spectra were recorded at 35 °C, where the DMPC lipids are in a fluid lamellar phase bilayer. H) 2D ^{1}H–^{15}N PISEMA spectrum of SMA-EA macro-nanodiscs containing ^{15}N-cytochrome b_5 reconstituted in DMPC lipid bilayers with the bilayer normal perpendicular to the external magnetic field. I) ^{31}P static NMR spectra of macro-nanodiscs with varying concentration of $YbCl_3$.

the ^{31}P peak appeared at around 20 ppm (Figure 4C) and the ^{14}N quadrupole coupling splitting increased by a factor of 2 to become about 16 kHz (Figure 4F); this change is according to the second-order polynomial, $^1/_2(3\cos^2\theta-1)$, in the quadrupole coupling Hamiltonian, where θ is the angle between the lipid bilayer normal and the magnetic field direction. Since the macro-nanodiscs are smaller than MLVs, the motionally averaged ^{31}P chemical shift anisotropy span should be smaller (unaligned ^{31}P lineshape is shown in Figure S8); in addition, the added lanthanide ions can affect the chemical shift values.[18] The ability to control the extent of flip of macro-nanodiscs is also demonstrated by recording ^{31}P spectra for various concentrations of Yb^{3+} (Figure 4I). The magnetic-alignment properties of lipid bilayers in macro-nanodiscs are similar to that has been reported for bicelles.[17,19] To our knowledge, this is the first study demonstrating the magnetic-alignment of lipid macro-nanodiscs.

It is remarkable that polymer-based macro-nanodiscs can be aligned in a magnetic field. Such aligned macro-nanodiscs enable the applications of well-established solid-state NMR experiments that have been used to obtain atomic-resolution images of membrane proteins in fluid lamellar phase lipid bilayers by measuring anisotropic NMR parameters such as chemical shift, heteronuclear dipolar couplings and quadrupole couplings.[20] One of the commonly used solid-state NMR techniques is 2D PISEMA (polarization inversion and spin exchange at magic angle) spectroscopy that has been well utilized in obtaining dynamic structure and topology of membrane proteins embedded in lipid bilayers.[21] Here, we demonstrate the feasibility of 2D PISEMA experiment using magnetically-aligned macro-nanodiscs containing a ^{15}N-labeled cytochrome b_5 protein as an example. The 2D PISEMA spectrum shown in Figure 4H correlates ^{15}N chemical shifts with ^1H–^{15}N dipolar couplings. Since cytochrome b_5 consists of a rigid transmembrane helix and a mobile large soluble domain, the resonances observed in the PISEMA spectrum mostly appear from the rigid transmembrane domain while the resonances from the soluble domain of the protein are motionally averaged out. The helical geometry of the transmembrane helix of cytb_5 gives rise to a characteristic "wheel"-like pattern of resonances in the 2D PISEMA spectrum. Simulation of the helical wheel pattern revealed that the transmembrane helix is tilted by $14.5 \pm 3°$ away from the lipid bilayer normal (Supporting Information Figure S10), which is in agreement with previous studies on magnetically-aligned bicelles.[22] These results demonstrate the feasibility of static solid-state NMR experiments to study membrane proteins reconstituted in macro-nanodiscs.

We also demonstrate the application of SMA-EA based nanodiscs for solution NMR studies on reconstituted membrane proteins. A 2D ^1H–^{15}N TROSY-HSQC (transverse relaxation optimized spectroscopy heteronuclear single quantum correlation)[23] NMR spectrum of ^{15}N-labeled cyt$b5$ is shown in Figure 4G. The high-resolution solution NMR spectrum indicates that the protein is well folded in agreement with a previous study[24] and therefore the application of well-developed multidimensional solution NMR techniques for high-resolution structural and dynamics studies are feasible using the SMA-EA polymer-based nanodiscs.

In conclusion, we have successfully overcome the difficulties in producing small-molecular-weight polymer based nanodiscs using a simple and inexpensive chemical reaction, and for the first time, polymer-based nanodiscs of varying size (10 to 50 nm) can be produced and used for reconstitution of a membrane protein for high-resolution structural studies by NMR spectroscopy. Our results are remarkable in that the SMA-EA-based macro-nanodiscs spontaneously align in an external magnetic field enabling the well-established solid-state NMR based structural and dynamics studies on membrane proteins, in addition to the commonly used multidimensional solution NMR experiments on SMA-EA nanodiscs[2] and MAS experiments[25] macro-nanodiscs. The reported experimental results provide valuable insights into the properties, structural assembly, and mechanism of formation of nanodiscs. Therefore, we foresee that the ease with which various-size SMA-EA nanodiscs/macro-nanodiscs can be prepared would dramatically expand the applications of polymer-based nanodiscs in various fields including structural biology, biotechnology, and biomedicine.

Acknowledgements

This study was supported by the NIH (GM084018 to A.R.). We thank Dr. Sang-Choul and Dr. Lucy Waskell for providing the plasmid and help with the preparation of cytochrome b_5.

Conflict of interest

The authors declare no conflict of interest.

Keywords: lipids · membrane proteins · nanodiscs · NMR spectroscopy · polymers

How to cite: *Angew. Chem. Int. Ed.* **2017**, *56*, 11466–11470
Angew. Chem. **2017**, *129*, 11624–11628

[1] R. Phillips, T. Ursell, P. Wiggins, P. Sens, *Nature* **2009**, *459*, 379–385.
[2] M. L. Nasr, D. Baptista, M. Strauss, Z. J. Sun, S. Grigoriu, S. Huser, A. Pluckthun, F. Hagn, T. Walz, J. M. Hogle, G. Wagner, *Nat. Methods* **2017**, *14*, 49–52.
[3] I. G. Denisov, S. G. Sligar, *Nat. Struct. Mol. Biol.* **2016**, *23*, 481–486.
[4] I. G. Denisov, S. G. Sligar, *Chem. Rev.* **2017**, *117*, 4669–4713.
[5] T. H. Bayburt, Y. V. Grinkova, S. G. Sligar, *Nano Lett.* **2002**, *2*, 853–856.
[6] T. H. Bayburt, Y. V. Grinkova, S. G. Sligar, *Arch. Biochem. Biophys.* **2006**, *450*, 215–222.
[7] F. Hagn, M. Etzkorn, T. Raschle, G. Wagner, *J. Am. Chem. Soc.* **2013**, *135*, 1919–1925.
[8] M. Zhang, R. Huang, R. Ackermann, S. C. Im, L. Waskell, A. Schwendeman, A. Ramamoorthy, *Angew. Chem. Int. Ed.* **2016**, *55*, 4497–4499; *Angew. Chem.* **2016**, *128*, 4573–4575; H. Kondo, K. Ikeda, M. Nakano, *Colloids Surf. B* **2016**, *146*, 423–430; S. H. Park, S. Berkamp, G. A. Cook, M. K. Chan, H. Viadiu, S. J. Opella, *Biochemistry* **2011**, *50*, 8983–8985.
[9] M. Orwick-Rydmark, J. E. Lovett, A. Graziadei, L. Lindholm, M. R. Hicks, A. Watts, *Nano Lett.* **2012**, *12*, 4687–4692; A. O. Oluwole, B. Danielczak, A. Meister, J. O. Babalola, C. Vargas, S.

Keller, *Angew. Chem. Int. Ed.* **2017**, *56*, 1919 – 1924; *Angew. Chem.* **2017**, *129*, 1946 – 1951.
[10] T. K. Ritchie, Y. V. Grinkova, T. H. Bayburt, I. G. Denisov, J. K. Zolnerciks, W. M. Atkins, S. G. Sligar, *Methods Enzymol.* **2009**, *464*, 211 – 231.
[11] J. M. Dörr, M. C. Koorengevel, M. Schafer, A. V. Prokofyev, S. Scheidelaar, E. A. van der Cruijsen, T. R. Dafforn, M. Baldus, J. A. Killian, *Proc. Natl. Acad. Sci. USA* **2014**, *111*, 18607 – 18612.
[12] S. C. Lee, T. J. Knowles, V. L. Postis, M. Jamshad, R. A. Parslow, Y. P. Lin, A. Goldman, P. Sridhar, M. Overduin, S. P. Muench, T. R. Dafforn, *Nat. Protoc.* **2016**, *11*, 1149 – 1162.
[13] M. C. Orwick, P. J. Judge, J. Procek, L. Lindholm, A. Graziadei, A. Engel, G. Grobner, A. Watts, *Angew. Chem. Int. Ed.* **2012**, *51*, 4653 – 4657; *Angew. Chem.* **2012**, *124*, 4731 – 4735.
[14] J. M. Dörr, S. Scheidelaar, M. C. Koorengevel, J. J. Dominguez, M. Schafer, C. A. van Walree, J. A. Killian, *Eur. Biophys. J.* **2016**, *45*, 3 – 21.
[15] S. Scheidelaar, M. C. Koorengevel, C. A. van Walree, J. J. Dominguez, J. M. Dorr, J. A. Killian, *Biophys. J.* **2016**, *111*, 1974 – 1986.
[16] C. R. Sanders, J. H. Prestegard, *Biophys. J.* **1990**, *58*, 447 – 460; U. H. N. Dürr, M. Gildenberg, A. Ramamoorthy, *Chem. Rev.* **2012**, *112*, 6054 – 6074.
[17] R. S. Prosser, S. A. Hunt, J. A. DiNatale, R. R. Vold, *J. Am. Chem. Soc.* **1996**, *118*, 269 – 270.
[18] R. S. Prosser, J. S. Hwang, R. R. Vold, *Biophys. J.* **1998**, *74*, 2405 – 2418.
[19] C. R. Sanders, B. J. Hare, K. P. Howard, J. H. Prestegard, *Prog. Nucl. Magn. Reson. Spectrosc.* **1994**, *26*, 421 – 444; A. A. De Angelis, A. A. Nevzorov, S. H. Park, S. C. Howell, A. A. Mrse, S. J. Opella, *J. Am. Chem. Soc.* **2004**, *126*, 15340 – 15341.
[20] F. M. Marassi, S. J. Opella, *J. Magn. Reson.* **2000**, *144*, 150 – 155; J. Wang, J. Denny, C. Tian, S. Kim, Y. Mo, F. Kovacs, Z. Song, K. Nishimura, Z. Gan, R. Fu, J. R. Quine, T. A. Cross, *J. Magn. Reson.* **2000**, *144*, 162 – 167.
[21] C. H. Wu, A. Ramamoorthy, S. J. Opella, *J. Magn. Reson. Ser. A* **1994**, *109*, 270 – 272; A. Ramamoorthy, C. H. Wu, S. J. Opella, *J. Magn. Reson.* **1999**, *140*, 131 – 140; A. Ramamoorthy, Y. Wei, D.-K. Lee, *Annu. Rep. NMR Spectrosc.* **2004**, *52*, 1 – 52.
[22] U. H. Dürr, K. Yamamoto, S. C. Im, L. Waskell, A. Ramamoorthy, *J. Am. Chem. Soc.* **2007**, *128*, 6670 – 6671.
[23] K. Pervushin, R. Riek, G. Wider, K. Wüthrich, *Proc. Natl. Acad. Sci. USA* **1997**, *94*, 12366 – 12371.
[24] S. Ahuja, N. Jahr, S. C. Im, S. Vivekanandan, N. Popovych, S. V. Le Clair, R. Huang, R. Soong, J. Xu, K. Yamamoto, R. P. Nanga, A. Bridges, L. Waskell, A. Ramamoorthy, *J. Biol. Chem.* **2013**, *288*, 22080 – 22095.
[25] L. S. Brown, V. Ladizhansky, *Protein Sci.* **2015**, *24*, 1333 – 1346; B. J. Wylie, M. P. Bhate, A. E. McDermott, *Proc. Natl. Acad. Sci. USA* **2014**, *111*, 185 – 190; M. Kaplan, C. Pinto, K. Houben, M. Baldus, *Q. Rev. Biophys.* **2016**, *49*, e15.

Manuscript received: May 31, 2017
Accepted manuscript online: July 16, 2017
Version of record online: August 10, 2017

